POLITECNICO DI TORINO
Repository ISTITUZIONALE

Fire Safety Analysis of Alternative Vehicles in Confined Spaces: A Study of Underground Parking Facilities

Original
Fire Safety Analysis of Alternative Vehicles in Confined Spaces: A Study of Underground Parking Facilities / Leone, E., Papurello, D.. - In: FIRE. - ISSN 2571-6255. - 9:1(2026). [10.3390/fire9010020]

Availability:
This version is available at: 11583/3006258 since: 2026-01-02T13:17:53Z

Publisher:
MDPI

Published
DOI:10.3390/fire9010020

Terms of use:

This article is made available under terms and conditions as specified in the corresponding bibliographic description in the repository

Publisher copyright

(Article begins on next page)

19 November 2026

fire

MDPI

Communication

Fire Safety Analysis of Alternative Vehicles in Confined Spaces: A Study of Underground Parking Facilities

Edoardo Leone [1] and Davide Papurello [1,2,*]

[1] Department of Energy, Politecnico di Torino, Corso Duca Degli Abruzzi 24, 10129 Turin, Italy
[2] Energy Center, Politecnico di Torino, Via Borsellino 38, 10138 Turin, Italy
* Correspondence: davide.papurello@polito.it

Abstract

This study investigates the fire behaviour of Battery Electric Vehicles (BEVs) and Internal Combustion Engine Vehicles (ICEVs) in confined environments such as underground parking facilities and tunnels. Using the Fire Dynamics Simulator (FDS), several scenarios were modelled to analyse the effects of ventilation and automatic suppression systems on fire growth, heat release, and smoke propagation. Three ventilation configurations—reduced, standard, and increased airflow—were evaluated to determine their influence on combustion dynamics and thermal development. Results show that BEV fires produce higher peak Heat Release Rates (up to 7 MW) and longer combustion durations than ICEVs, mainly due to self-sustained battery reactions. Increased ventilation enhances smoke removal but intensifies flames and radiant heat transfer, while limited airflow restricts combustion yet leads to hazardous smoke accumulation. The inclusion of a sprinkler system effectively reduced temperatures by over 60% within 100 s of activation, though residual heat in BEVs poses a risk of re-ignition. This underlines the need for tailored ventilation and suppression strategies in modern underground facilities to ensure safety in the transition toward electric mobility.

Keywords: BEVS; Li-ion; thermal runaway; underground car park; fire; shutdown; sprinklers; FDS; CFD

1. Introduction

The global transition towards sustainable mobility has accelerated the adoption of electric and hybrid vehicles, profoundly reshaping the automotive sector and posing new challenges for fire safety engineering. As electric and hybrid vehicles become increasingly common in road networks, attention has shifted to understanding their behaviour in critical environments such as underground parking facilities. These confined infrastructures are characterised by limited ventilation, restricted access for firefighting operations, and complex evacuation dynamics, which can amplify the consequences of vehicle fires [1,2]. Battery Electric Vehicles (BEVs) rely on high-energy lithium-ion battery (LIB) systems that, while efficient and compact, introduce unique safety concerns compared to conventional internal combustion engine vehicles (ICEVs). Fires involving BEVs differ in both origin and development [3–5]. Whereas ICEV fires are generally linked to the ignition of liquid fuels, BEV incidents often arise from thermal runaway—a chain reaction initiated by mechanical impact, electrical failure, or overheating, which leads to uncontrolled exothermic reactions within the battery cells [6–8]. During such events, internal temperatures may exceed 800 °C, accompanied by the release of flammable and toxic gases

Check for updates

Academic Editors: Jason Gill, Simon Lambert and Gongquan Wang

Received: 14 November 2025
Revised: 12 December 2025
Accepted: 23 December 2025
Published: 29 December 2025

Copyright: © 2025 by the authors. Licensee MDPI, Basel, Switzerland. This article is an open access article distributed under the terms and conditions of the Creative Commons Attribution (CC BY) license.

such as hydrogen fluoride (HF), carbon monoxide (CO), and hydrocarbons, significantly increasing the risks to first responders and occupants in confined spaces [6,9]. Experimental fire tests conducted at facilities such as Zentrum am Berg (Austria) have shown that BEV fires can produce heat release rates (HRR) comparable to or even exceeding those of conventional vehicles, typically ranging between 6 and 8 MW [2]. However, unlike ICEV fires, which depend on the presence of atmospheric oxygen, BEV fires can sustain themselves internally due to oxygen release from cathode decomposition, making extinguishment considerably more difficult [10–12]. In addition, the risk of re-ignition remains high even after apparent fire suppression, often requiring prolonged cooling or complete submersion of the vehicle in water to prevent recurrence [13–15]. Recent large car-park fires and the rapid evolution of vehicle technology have triggered a surge of international research on fire loads, fire spread between vehicles and the adequacy of traditional design fires in parking structures [16–18]. Miechówka et al. compiled 148 full-scale car fire experiments from 44 sources into a structured database, providing up-to-date statistical distributions of HRR, THR and time-to-peak specifically for use in car-park design fires [17]. Olenick et al., quantitatively compared the fire risks of modern vehicles with the assumptions made in the standards and showed that the current protection requirements for multi-storey car parks may be overly conservative or insufficient, particularly for scenarios involving the spread of fire to multiple vehicles [19]. Tohir et al., studied the spread of fire to multiple vehicles in car parks using a probabilistic approach, considering the different HRR graphs [20]. Park et al., conducted large-scale calorimetric tests on fires involving one or two vehicles, quantifying the HRR, smoke and toxic gas production, and demonstrating how the distance between vehicles affects the spread of fire from one vehicle to another [21]. Zhu et al. reported the results of large-scale vehicle fire tests conducted in a simulated underground car park, providing detailed data on temperature, flame propagation and smoke layer that can be directly used to validate CFD models and smoke control designs [22].

Given the complexity of these phenomena, numerical modelling has become an essential tool for assessing fire behaviour and smoke propagation in confined infrastructures. Computational Fluid Dynamics (CFD) tools such as Fire Dynamics Simulator (FDS) have been widely adopted to simulate BEV and ICEV fires under varying ventilation conditions, allowing researchers to quantify differences in temperature distribution, visibility, and heat release rate per unit area (HRRPUA) [11,23–28]. In parallel, several stakeholders (e.g., NFPA's Fire Protection Research Foundation, the European Fire Safety Alliance and Euralarm) are developing and refining guidance and classification frameworks for modern-vehicle hazards, sprinkler and detection requirements, and operational strategies specific to car parks with high shares of EVs and hybrids [29,30]. At policy level, recent EU guidance for covered parking areas and indoor car parks translates this evidence base into practical recommendations on prevention, detection, evacuation, structural/passive protection and firefighting. Despite substantial progress, several knowledge gaps remain. The scalability of thermal runaway events in large battery packs, the interaction between multiple burning vehicles, and the long-term integrity of structural materials exposed to BEV fires require further investigation. A comprehensive understanding of these aspects is crucial for developing updated safety standards and emergency response strategies that reflect the evolving composition of vehicle fleets.

This study contributes to this effort by analysing the thermal behaviour of alternative vehicles and evaluating their fire dynamics in confined environments through both experimental data and CFD-based modelling.

2. Material and Methods—Simulation

The research methodology is based exclusively on numerical simulations performed using the Fire Dynamics Simulator (FDS), a Computational Fluid Dynamics (CFD) code developed by the National Institute of Standards and Technology (NIST, US). The modelling approach aims to reproduce realistic fire scenarios, evaluate the heat release characteristics of BEVs and ICEVs, and assess the influence of ventilation and automatic extinguishing systems on the evolution of fire and smoke in confined spaces.

2.1. Simulation Environment and Model Design

The geometrical models were designed using standard dimensional references and construction features typically found in European infrastructure. The underground car park was modelled as a rectangular enclosure measuring 16 × 15 × 2.4 m, containing multiple vehicles aligned in two rows with standard spacing (0.8 m, corresponding to EU parking layout guidelines), see Figure 1 [31].

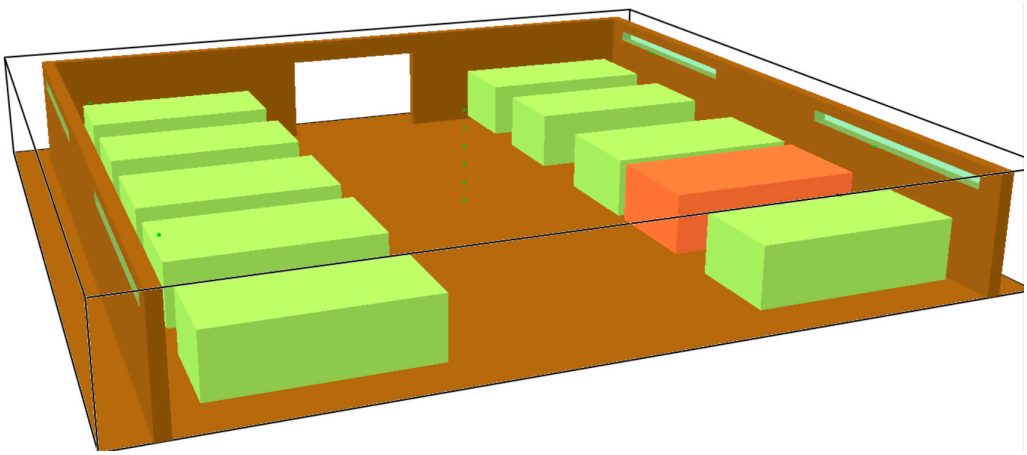


Figure 1. Structure of the underground parking with the vehicles (green, non-primary vehicles–orange vehicle, active vehicle).

Two different materials were defined: the "BRICK" with characteristics similar to concrete (density (1600–2000 kg/m^3), thermal conductivity (0.7–0.9 W/mK), specific heat capacity (800–1000 J/kgK)) [32] for the definition of the walls defined as 'WALL' surfaces, and the 'car_mat' (density (900–1600 kg/m^3), thermal conductivity (0.2–0.4 W/mK), specific heat capacity (1200–2000 J/kgK) [33]) to define the characteristics of the vehicles, and their relative surface. These thermophysical properties govern how quickly the vehicle surfaces absorb and re-emit heat, thereby influencing both the rate of flame spread across the car body and the magnitude of radiative feedback that drives fire growth. Then, the walls, the entrance, the windows, the open surfaces and finally, the position of the vehicles were defined with the appropriate parameters and conditions. The role of the concrete structure is to represent the thermal inertia of the car park roof and influence heat absorption and gas release behaviour. The side openings are defined in different modes depending on the ventilation condition, which will affect the spread of fire and smoke circulation. Closed windows on reduced ventilation, open on increased ventilation and for the standard case, the windows will explode when the temperature reaches 300 °C; this ideally represents the cracking of the glass in the side openings that would occur in real conditions around that temperature. The environment was discretised using a uniform computational mesh suitable for transient calculations, allowing an accurate representation of temperature gradients, smoke propagation, and ventilation effects. The computational domain was discretised using a uniform 0.30 m mesh, resulting in roughly 57,600 cells. Mesh quality

checks confirmed acceptable aspect ratios and overall geometric fidelity. A mesh-sensitivity study, carried out following NIST guidelines, compared the 10 cm grid with a refined 7.5 cm mesh [34]. Differences in predicted HRR and ceiling temperatures were below 5%, indicating that the selected 0.30 m resolution was sufficient for accurate simulation. The simulation time was set to 1200 s for the parking scenario. This duration was selected to represent the average fire growth and intervention times reported in the literature.

Three different ventilation conditions were analysed for the parking case:

- Reduced ventilation, with limited air exchange and closed lateral openings. In this configuration, all side openings were kept closed, and air exchange occurred only through minimal leakage and the main entrance area (6 m^2). This condition represents a worst-case scenario where oxygen availability is limited, leading to incomplete combustion and rapid smoke accumulation beneath the ceiling. The lack of fresh air inflow caused the fire to become oxygen-limited after a short growth phase.
- Standard ventilation, with windows breaking at approximately 300 °C, simulating glass failure [35]. In the baseline configuration, the side windows were initially closed but programmed to break automatically when the local temperature reached 300 °C, simulating the thermal cracking of glass observed in real fires. This dynamic event introduced natural ventilation at mid-height, allowing partial air exchange between the interior and exterior. The resulting airflow helped stabilise the combustion process and delayed full smoke saturation, providing a realistic representation of typical underground parking conditions.
- Increased ventilation, with side openings kept open throughout the simulation. In this case, the lateral openings were kept open from the start of the simulation, enabling continuous air exchange. The total effective opening area was approximately 20 m^2 (four side windows of 5 m^2 each), supplemented by the 6 m^2 entrance. This produced stronger natural convection currents, improving smoke removal but also enhancing flame intensity due to the higher oxygen supply. The airflow induced by temperature-driven buoyancy and pressure differences generated turbulent circulation patterns that increased radiant heat transfer to adjacent vehicles.

2.2. Fire Source Definition and Input Parameters

The fire source was defined based on full-scale experimental data available in the literature, ensuring that the simulated heat release characteristics accurately represent realistic vehicle fire behaviour. The Heat Release Rate (HRR) values for each vehicle type were derived from combustion experiments performed at the Zentrum am Berg (ZaB) tunnel research facility [2]. Heat Release Rate (HRR) is the rate at which heat energy is released by a fire and is a fundamental metric for quantifying fire intensity and growth in combustion processes, commonly expressed in watts and assessed through methods such as oxygen-consumption or mass-loss measurements [36]. The HRR can be related to the burning rate of material by the formula:

$$\mathrm{HRR} = \dot{m}\,\Delta h_c, \tag{1}$$

where $\dot{m}$ is the mass loss rate of the combusting fuel and Δh_c is its effective heat of combustion, linking the chemical energy release to the fire's power output.

BEVs were assigned a maximum HRR of 7 MW, while ICEVs were set at 5 MW, corresponding to Heat Release Rates per Unit Area (HRRPUA) of 219 kW/m^2 and 156 kW/m^2, respectively. These values represent average peak conditions derived from combustion experiments of passenger vehicles conducted at the Zentrum am Berg (ZaB) tunnel research facility. The initial data are those related to Figure 8 of the publication [2]. Using the HRR peak ensures a conservative approach to fire safety assessment, as it reflects the moment

when the vehicle releases maximum thermal power and therefore places the most severe load on ventilation systems, compartmentalisation criteria and escape routes. The heat release curve followed a typical t-square growth rate, increasing linearly to the peak HRR within the first 300–400 s and subsequently stabilising near the plateau phase. The model assumed constant HRR during the fully developed stage, followed by a gradual decline to replicate energy depletion. Each vehicle was modelled as a volumetric heat source located within the domain according to the car park geometry described in Section 2.1. The ignition point was defined on the reference vehicle (highlighted in orange in Figure 1), initiating the combustion process through a localised thermal input consistent with observed ignition modes in real BEV fires.

2.3. Fire Suppression Modelling

To assess the influence of active fire protection systems, an automatic sprinkler network was incorporated into the numerical model. The configuration was designed to reproduce the operation of a conventional suppression system commonly installed in underground parking facilities, where early control of flame spread and heat accumulation is critical for occupant safety and structural integrity. The system comprised three ceiling-mounted nozzles positioned along the central axis of the car park. Each nozzle was assigned a discharge flow rate of 80 L/min and an ejection velocity of 10 m/s, values representative of standard high-pressure sprinkler systems used in confined infrastructures. The sprinklers were activated 500 s after ignition, corresponding to the typical delay between fire onset and the initiation of suppression in real-world underground scenarios. A fixed activation time of 500 s was adopted as a representative delay for underground car-park scenarios and to ensure a consistent, directly comparable suppression onset across all simulated ventilation conditions. In addition to the discharge range and ejection velocity, the sprinkler spray was characterised by a predefined droplet distribution based on a representative Sauter mean diameter for fine mist irrigation systems. The droplets were released at an initial velocity of 10 m/s and distributed in a conical spray pattern, with an injection angle selected to ensure complete coverage of the ignition vehicle and the surrounding area.

Water dispersion was modelled using the spray functionality of the Fire Dynamics Simulator (FDS), which allows the interaction between evaporating droplets and the surrounding hot gases to be resolved. The spray was introduced as a distribution of fine droplets across the upper domain, producing a dual effect: Thermal attenuation, achieved through convective heat absorption and phase change, which reduced the temperature of the combustion gases; and oxygen displacement, caused by the generation of steam, locally decreased oxygen concentration and limited flame stability.

The simulation enabled the quantification of sprinkler performance by monitoring the heat release rate (HRR), temperature decay, and smoke layer development following activation. The analysis focused particularly on the transient period immediately after water discharge, allowing evaluation of suppression efficiency under varying ventilation conditions. The primary output variables included Heat Release Rate (HRR), temperature distribution, gas flow velocity, smoke density, and visibility. These parameters were extracted at multiple heights and locations to assess the development of fire and smoke stratification under different ventilation and suppression conditions. The visualisation of flame propagation, temperature fields, and smoke movement was carried out using Smokeview, the post-processing tool associated with FDS.

3. Results and Discussion—Underground Parking

The numerical analysis of the underground parking configuration provided a detailed understanding of the fire evolution, smoke propagation, and thermal effects gen-

erated by both Battery Electric Vehicles (BEVs) and Internal Combustion Engine Vehicles (ICEVs). In the model, the vehicle highlighted in orange could be configured to represent either a BEV or an ICEV, allowing direct comparison under identical geometrical and boundary conditions. However, the detailed Fire Dynamics Simulator (FDS) and Smokeview visualisations—showing temperature evolution, flame propagation, and smoke distribution—are presented for the BEV configuration only. The results for the ICEV case are summarised in the final comparative figure illustrating the Heat Release Rate (HRR) trends for both vehicle types.

3.1. Fire Development

During the simulation, ignition was assumed to occur at the orange vehicle, initiating a localised combustion process that expanded within the first 300 s. Figure 2 illustrates the early development of flames during the BEV fire in the underground car park, approximately 75 s after ignition. These align with prior full-scale experiments that describe rapid flame growth and localised heat accumulation typical of lithium-ion battery fires [4,5,7]. The simulation shows that combustion initially concentrates around the ignition vehicle (highlighted in orange), producing intense localised flames that rapidly grow in height and spread laterally due to radiant heat feedback. At this stage, the flame front reaches the ceiling zone, where local temperatures begin to exceed 600 °C. The confined geometry of the parking space enhances the upward movement of hot gases, intensifying the flame–ceiling interaction and initiating early smoke layer formation. Figure 3 presents the temporal evolution of smoke propagation in the same scenario at (a) 150 s, (b) 400 s, and (c) 600 s after ignition. In panel (a), a dense smoke layer begins to form near the ceiling, reducing visibility to below 2 m. The smoke propagation patterns are consistent with CFD-based studies of confined-space fires with similar ceiling-layer stratification and reduction in visibility [11,23,27]. By 400 s (panel b), the smoke layer thickens, filling approximately 40–50 % of the room's volume under standard ventilation conditions, while temperatures in the upper region exceed 700 °C. At 600 s (panel c), the smoke plume reaches full stratification, with turbulent flow patterns and recirculation zones caused by side openings and ventilation effects. The dark, dense nature of the smoke—typical of polymer and electrolyte combustion—indicates the release of soot and toxic gases. This figure clearly demonstrates how limited ventilation in underground spaces exacerbates smoke accumulation, posing severe challenges for occupant evacuation and firefighting operations.

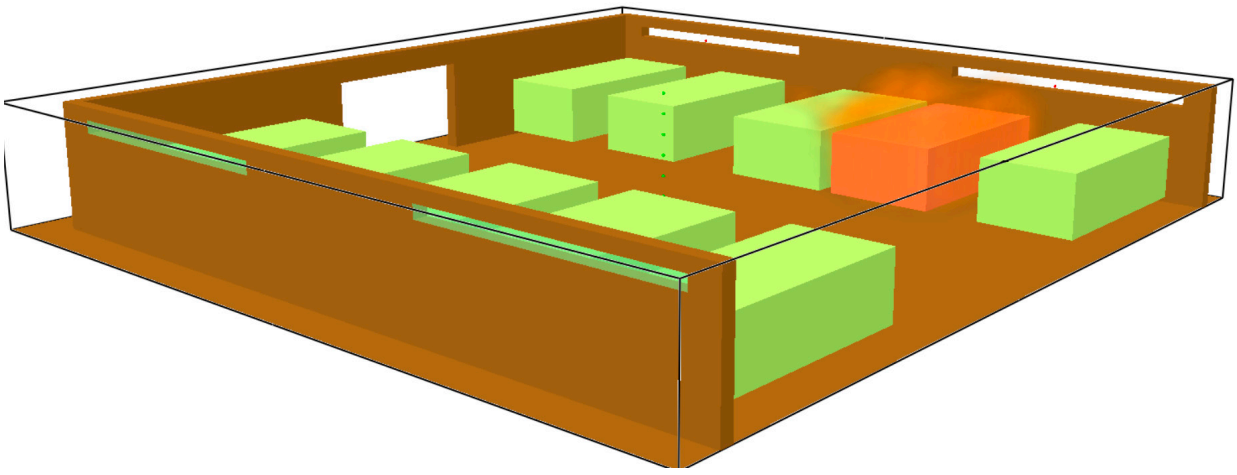


Figure 2. Detail of the development of flames (BEV)—75 s after the fire ignition.

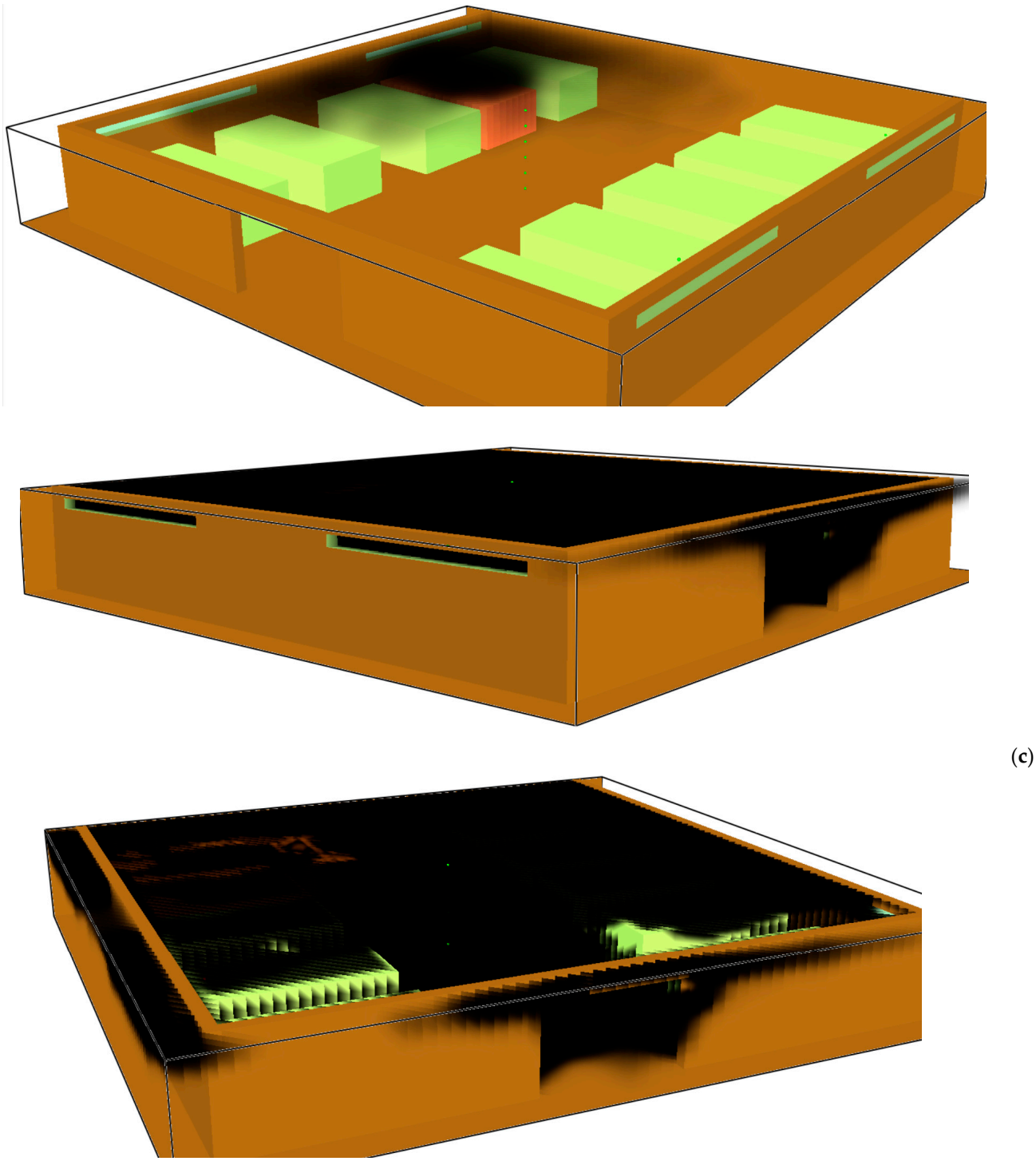


Figure 3. Development of smoke in the environment at the beginning of combustion of the development of flames (BEV)—(**a**) 150 s, (**b**) 400 s and (**c**) 600 s after the fire ignition.

Temperature contours revealed that the highest thermal loads developed directly above the orange vehicle, where ceiling temperatures reached 600–700 °C, with local peaks surpassing 800 °C for the BEV, see Figure 4.

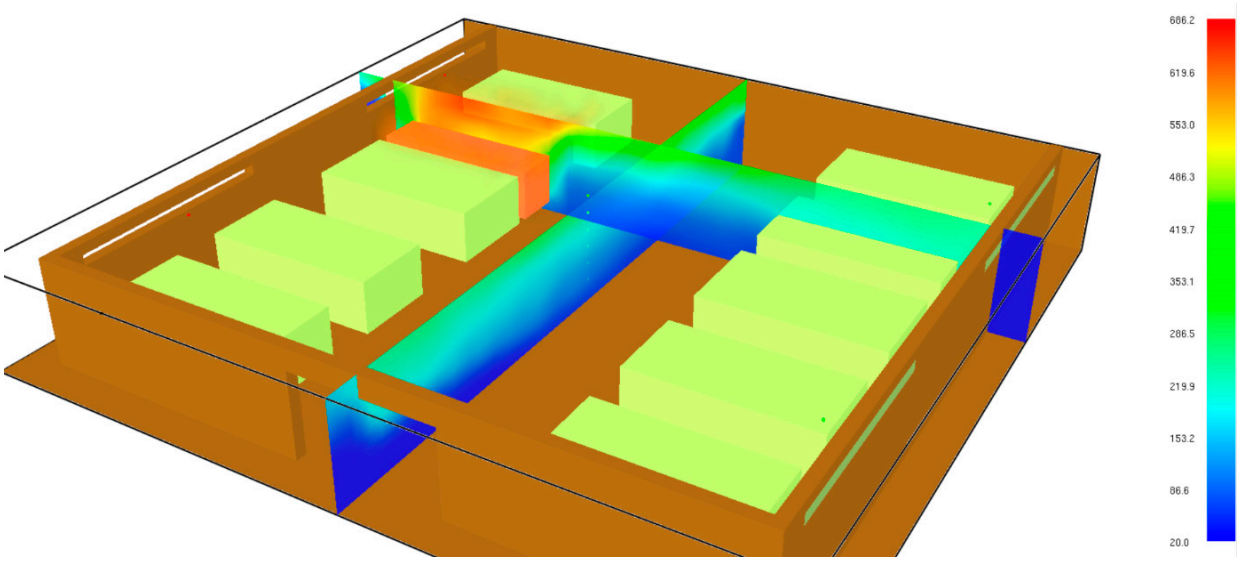


Figure 4. Development of temperature in the environment after 1135 s after the fire ignition for a BEV.

The fire propagation from the BEV shown above spreads to the nearest vehicle, see Figure 5.

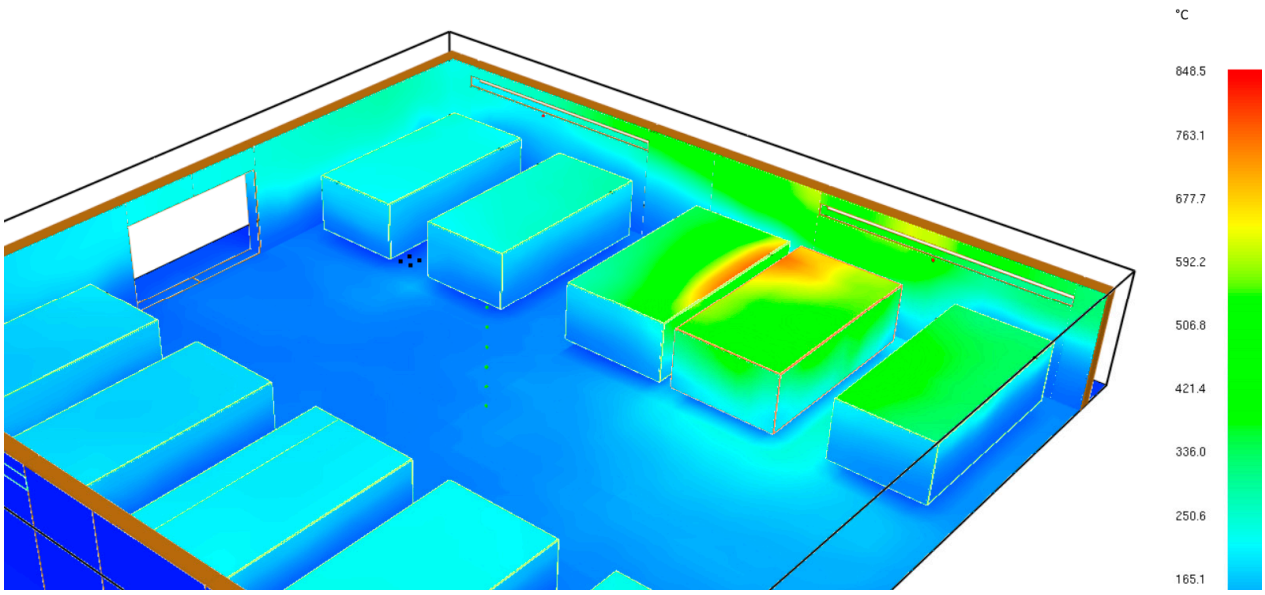


Figure 5. Display of adiabatic surfaces to detect the development and spread of the fire after 1125 s after the fire ignition for a BEV.

Figure 5 illustrates the spatial progression of the fire and the spread of thermal effects across vehicle surfaces in the underground car park at 1125 s after ignition. The visualisation of adiabatic surfaces highlights the zones exposed to the highest heat fluxes and radiant energy. The simulation shows that, by this stage, the fire originating from the initial Battery Electric Vehicle (BEV) has propagated to the nearest adjacent vehicle, confirming the potential for secondary ignition in confined parking layouts. The thermal contours indicate that radiant heat from the burning BEV significantly contributes to the ignition of neighbouring surfaces, with localised temperatures exceeding 800 °C near the ceiling. This progression underlines the influence of close vehicle spacing on fire escalation and demonstrates the persistence of BEV combustion even after the initial peak heat release rate. The fire spread illustrated in Figure 5 further confirms the findings of Brzezinska and Bryant, who observed secondary ignition risks in tightly spaced vehicles within

enclosed facilities [24]. The figure effectively visualises how sustained energy release and radiative transfer drive multi-vehicle involvement in confined car park fires, emphasising the challenges of fire containment and the need for rapid suppression systems [24].

3.2. Effect of the Ventilation Strategy

The influence of ventilation on fire development in the underground car park was examined under three distinct configurations: reduced, standard, and increased ventilation. Each configuration significantly affected the combustion dynamics, temperature distribution, and smoke propagation, revealing the complex interplay between oxygen availability, heat transfer, and confined-space aerodynamics. Under reduced ventilation, all lateral openings were kept closed, allowing air exchange only through the main entrance (6 m^2). The limited oxygen supply quickly led to an oxygen-depleted environment, constraining combustion but intensifying smoke accumulation. During the early growth phase (up to 300 s), the Heat Release Rate (HRR) rose moderately, followed by a premature decline as oxygen levels dropped. Although peak HRR values were lower (approximately 4 MW for BEV and 3.5 MW for ICEV), the confined gases reached high ceiling temperatures exceeding 300 °C, producing dense smoke layers that severely reduced visibility within 200 s. This configuration represents a worst-case scenario for occupant evacuation and firefighter intervention, as smoke stratification and toxic gas concentration increased rapidly while the combustion zone remained thermally active. In the standard ventilation condition, glass panels were programmed to fail at around 300 °C, simulating realistic window breakage during a fire. This introduced mid-height openings that improved air circulation and allowed partial oxygen replenishment. As shown in Figure 6, this condition produced a more stable combustion regime for both vehicle types. The HRR of the BEV fire reached approximately 5.8 MW, while the ICEV stabilised around 4.3 MW (see Figures 6 and 7). The fire reached a quasi-steady state where oxygen inflow balanced the combustion rate, limiting further escalation but sustaining a prolonged high-temperature environment. Temperature contours during this regime revealed ceiling temperatures above 600 °C, consistent with values reported in experimental full-scale tests in confined spaces.

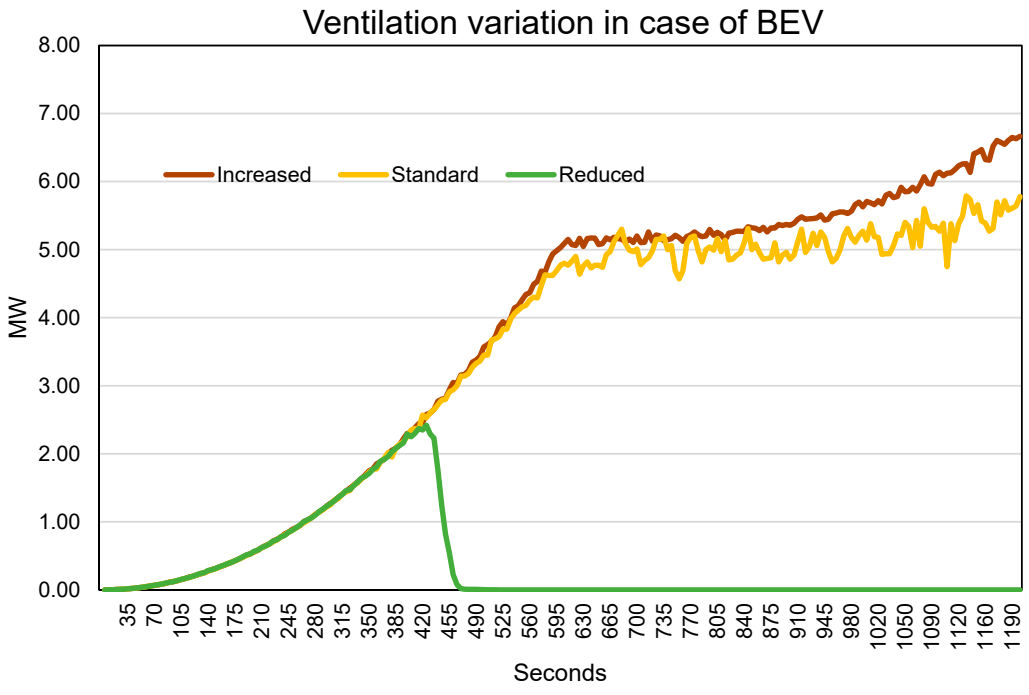


Figure 6. HRR released in case of BEV vs. Ventilation strategy.

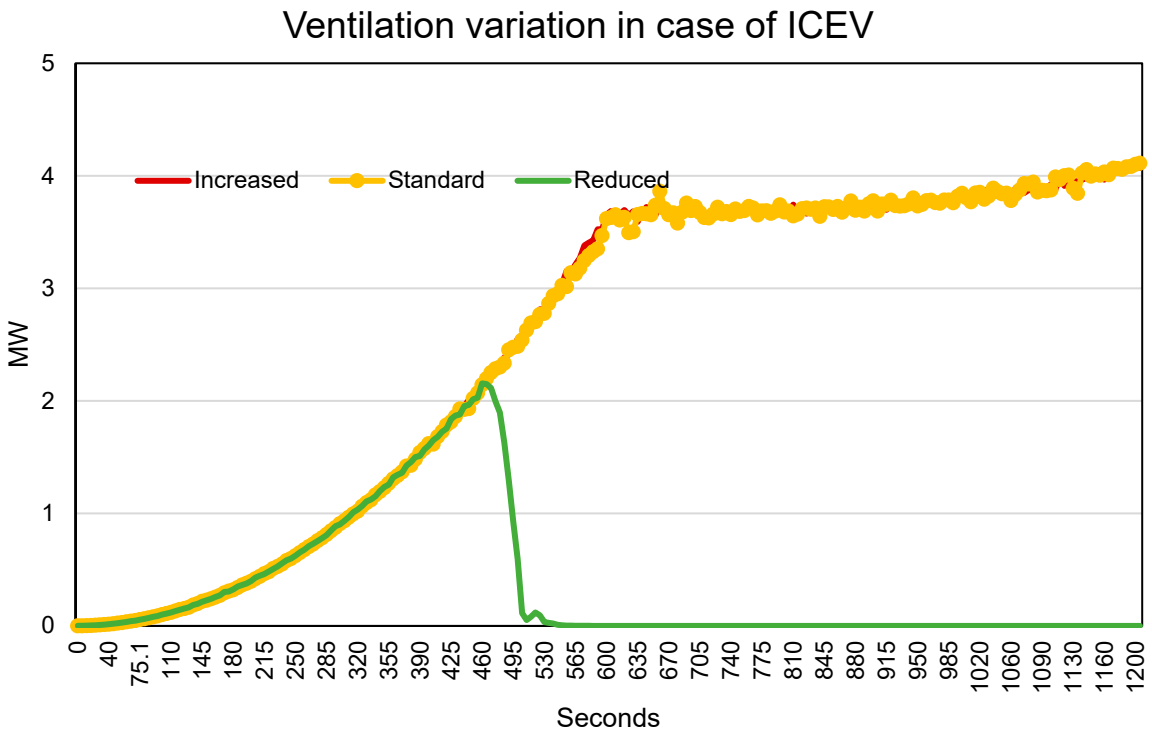


Figure 7. HRR released in case of ICEV vs. Ventilation strategy.

The increased ventilation case, in which all lateral openings were open from the start of the simulation (effective opening area ≈ 26 m^2), yielded the most intense fire dynamics. Enhanced oxygen availability sustained vigorous combustion, resulting in higher peak HRR values—up to 7 MW for BEV and 5 MW for ICEV—along with stronger turbulent mixing and flame spread. While this configuration facilitated faster smoke removal and delayed ceiling-layer saturation, it also significantly increased flame intensity and radiant heat transfer to adjacent vehicles. The interaction between buoyancy-driven convection and the airflow through open boundaries created highly turbulent recirculation zones that promoted secondary ignition.

The comparative HRR profiles across the three ventilation modes (Figure 6) highlight these trends. For BEVs, the HRR curve under increased ventilation (red) exhibits the highest peak and most sustained plateau, while the reduced-ventilation case shows an early saturation caused by oxygen deficiency. The difference between standard and increased ventilation reached approximately 1 MW, confirming that higher airflow enhances flame energy output. However, due to the self-sustaining nature of lithium-ion battery combustion, BEV fires under low-oxygen conditions did not extinguish as quickly as ICEV fires, deviating slightly from typical oxygen-dependent behaviour. This limitation reflects the model's inability to fully capture internal oxygen generation during thermal runaway, which would likely sustain combustion even under restricted ventilation. Figure 7 presents similar results for ICEVs, showing that combustion in conventional engines is far more sensitive to oxygen availability. The HRR values decline sharply under reduced ventilation, confirming the direct dependence of fuel combustion on external air supply. Unlike BEVs, no secondary heat peaks were observed, and the combustion plateau remained shorter and less intense.

Finally, Figure 8 compares BEV and ICEV behaviour under standard ventilation, the most representative real-world configuration. The BEV curve shows both a higher and more prolonged HRR plateau, averaging 1.5–2 MW greater than that of the ICEV throughout the steady phase. The simulation results (Figures 6–8) corroborate the patterns identified in

studies by Lan et al. [23] and Qiao et al. [26], showing that higher airflow enhances heat release while aiding smoke extraction [23,26].

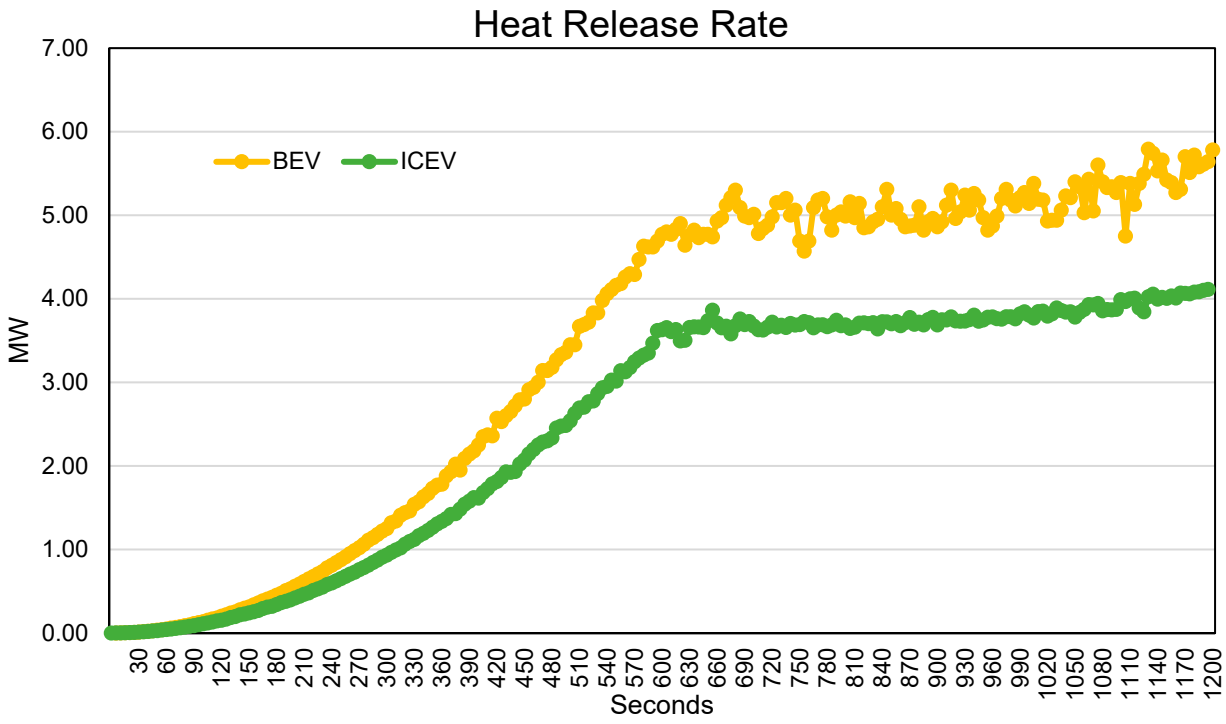


Figure 8. Comparison of HRRs of a BEV and an ICEV in the case of standard ventilation.

The BEV also displayed a minor secondary HRR rise near the end of the 1200 s simulation, corresponding to the ignition of adjacent surfaces—an indication of radiative and convective heat transfer sufficient to promote secondary fires in confined parking layouts.

Overall, these findings demonstrate that ventilation intensity plays a multiple role:

Improved ventilation enhances smoke removal and delays asphyxiation conditions but also increases flame intensity and accelerates fire spread. Restricted ventilation reduces combustion rate, traps smoke and heat, worsening evacuation conditions. The standard ventilation configuration offers a balanced compromise, maintaining tenable conditions longer while avoiding excessive heat buildup.

3.3. Fire Suppression

The suppression analysis focused on evaluating the performance of an automatic sprinkler system in mitigating fire growth within the underground car park under different ventilation conditions. Three ceiling-mounted sprinklers were activated 500 s after ignition, corresponding to the typical delay between fire onset and intervention in real underground scenarios. Each nozzle discharged water at 80 L/min with an ejection velocity of 10 m/s, ensuring uniform coverage of the fire zone. Figure 9 illustrates the start of the sprinkler activation at 520 s. At this stage, the fire—originating from the Battery Electric Vehicle (BEV)—had reached a fully developed phase, with a steady Heat Release Rate (HRR) of around 6–7 MW and ceiling temperatures approaching 800 °C. The ignition of the water jets produced immediate interaction with the hot gases, leading to rapid steam formation and localised cooling. The vapour cloud that developed near the ceiling partially displaced oxygen, attenuating the combustion process. Within the following 100 s, the combined thermal absorption and oxygen dilution effects of the sprinkler system produced a marked decrease in both temperature and flame intensity.

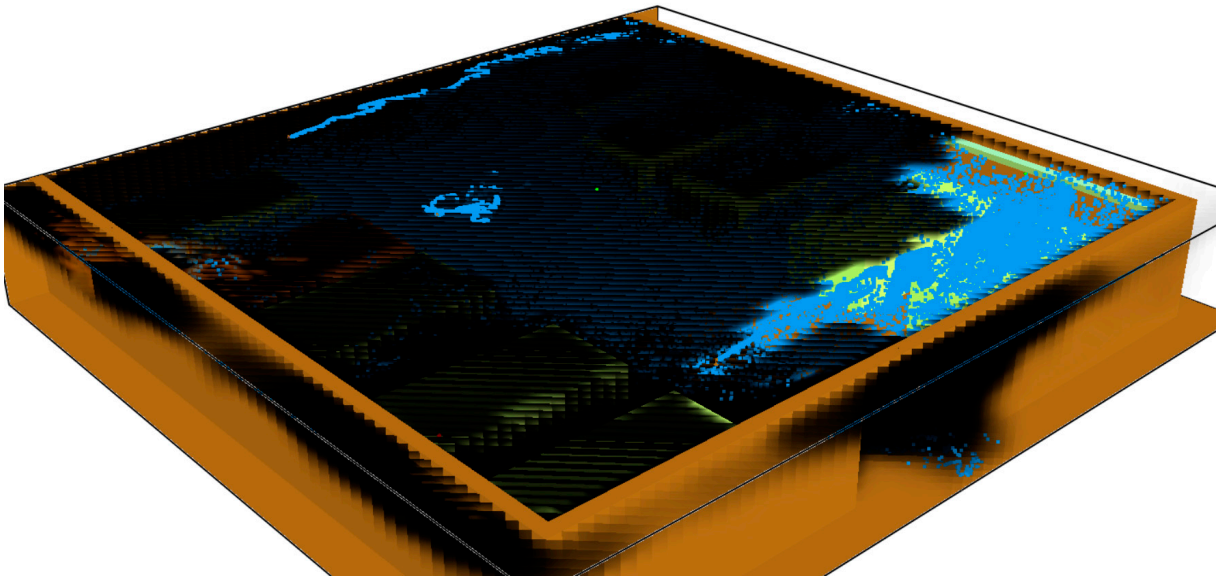


Figure 9. Start of the sprinkler system in the car park (520 s).

Figure 10 shows the car park 100 s after sprinkler activation (620 s total simulation time). The visualisation highlights a significant reduction in visible flames and smoke density, with temperatures in the upper layer decreasing by approximately 60 %. The water spray efficiently disrupted the flame front, cooled the ceiling layer, and slowed radiant heat transfer to adjacent vehicles—preventing secondary ignition that had been observed in the unsuppressed case. The effectiveness of the sprinkler system (Figures 9–11) aligns with previous CFD and experimental research demonstrating that water-based suppression can rapidly cool gases and interrupt combustion in confined spaces [11,24,27].

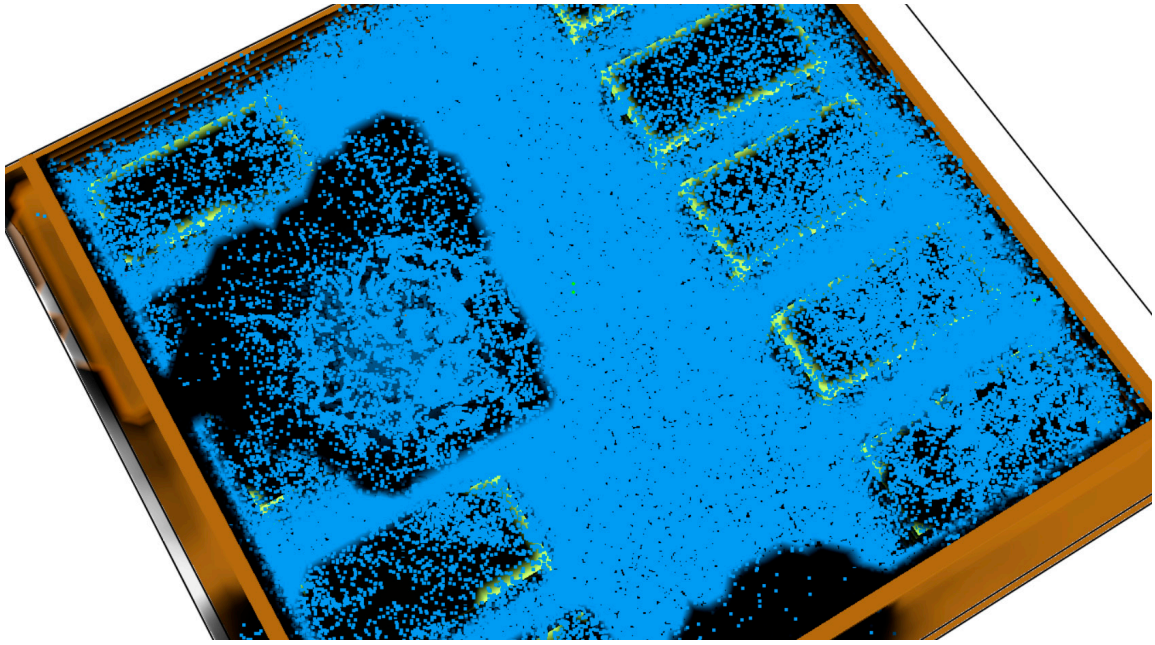


Figure 10. Effect of the sprinkler system in the car park (620 s).

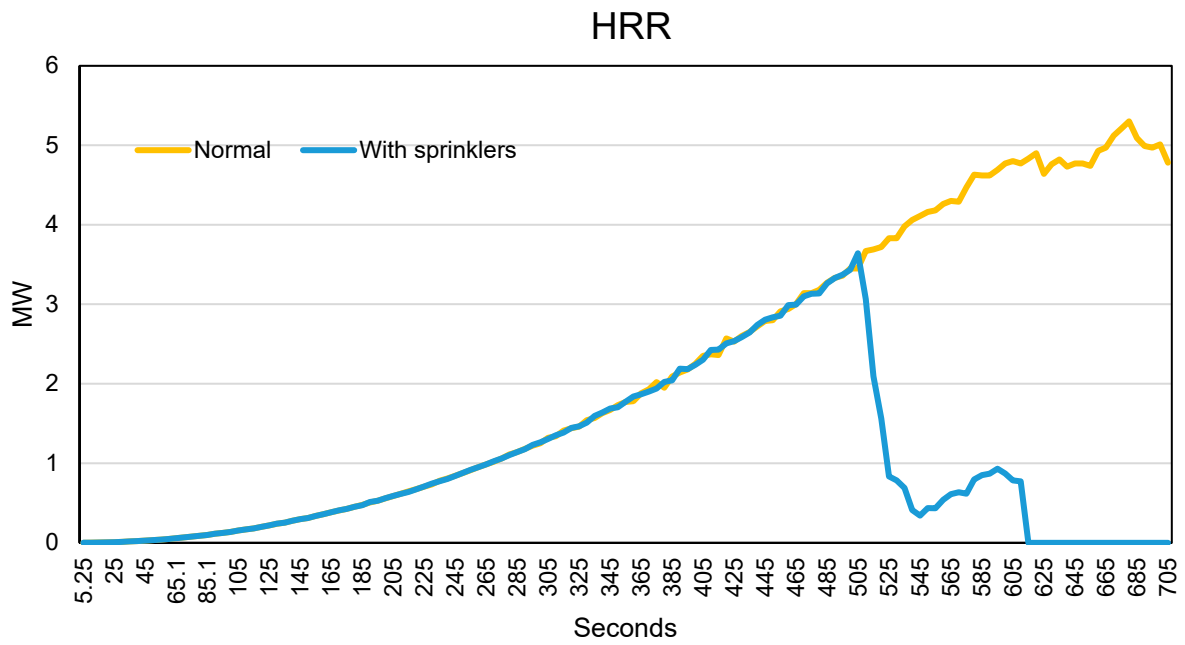


Figure 11. Comparison of the HRR of a BEV in the standard case without the extinction system and with the effect of the extinction system.

The suppression effect is quantitatively represented in Figure 11, which compares the HRR curves for the BEV fire under standard ventilation, with and without sprinkler intervention. In the uncontrolled case, HRR stabilised near 6.8 MW, maintaining high temperatures and continuous combustion. In contrast, the activation of the sprinkler system caused a sharp HRR collapse immediately after 520 s, dropping below 1 MW within approximately 100 s. The corresponding temperature profile followed the same trend, confirming the high efficiency of water-based suppression in reducing the energy output and flame intensity. By 620 s, combustion was nearly extinguished, and the environment transitioned into a cooling phase dominated by steam generation and gradual smoke clearance.

These results demonstrate that the sprinkler system was able to rapidly suppress the BEV fire, highlighting its effectiveness even in oxygen-rich environments. However, as supported by prior studies [8], residual heat within the battery modules can sustain internal exothermic reactions, posing a risk of re-ignition after apparent extinguishment. Therefore, extended cooling or complete submersion remains necessary for full suppression in post-fire management. From a comparative perspective, BEV fires showed more intense and persistent combustion than ICEV fires before suppression, owing to higher internal energy density and self-sustained reactions. Nevertheless, once activated, the sprinkler system produced similar relative reductions in HRR for both vehicle types, confirming that early intervention significantly limits heat accumulation and fire propagation in confined environments. Overall, the results presented in Figures 6–8 confirm that:

- Early sprinkler activation is critical for limiting fire spread and protecting adjacent vehicles.
- Water spray cooling and steam displacement are effective mechanisms for temperature reduction and oxygen suppression.
- Residual heat management is crucial for BEVs due to possible re-ignition.

4. Conclusions

This study provides new insight into the fire behaviour of Battery Electric Vehicles (BEVs) and Internal Combustion Engine Vehicles (ICEVs) in confined parking environments by examining not only peak Heat Release Rates, but also the combined influence of ventilation intensity, smoke movement, and suppression timing on fire development. Unlike previous work that mainly compares vehicle types in open or semi-open configurations, the present analysis quantifies how realistic boundary conditions of underground car parks alter BEV and ICEV fire dynamics and the associated risk of multi-vehicle involvement.

The results show that the ventilation strategy fundamentally changes fire progression. Increased ventilation enhances plume stability, raises the HRR plateau, and significantly accelerates thermal exposure to neighbouring vehicles—highlighting a mechanism of fire escalation not always recognised in BEV-related studies. Conversely, reduced ventilation lowers energy release but produces untenable conditions much earlier due to rapid smoke accumulation. These findings demonstrate that ventilation cannot be evaluated solely in terms of combustion rate: its dual impact on heat release and tenability conditions is critical for safety assessments.

The simulations also reveal that BEV fires in confined spaces generate sustained thermal loads that persist longer than those of ICEVs, even when HRR peaks are comparable. This prolonged energy release increases the likelihood of secondary ignition, underlining the importance of considering fire duration, not only HRR magnitude, in car-park fire-safety design. The modelling provides visual and quantitative evidence of how the thermal plume interacts with the car-park ceiling and adjacent vehicles—information rarely documented in underground-fire studies.

Concerning suppression, the analysis highlights that sprinkler activation, even when introduced at a fixed time, is capable of rapidly reducing temperatures and preventing fire spread. Importantly, however, the study confirms that suppression does not eliminate the internal energy source of a BEV in thermal runaway, meaning that re-ignition remains a credible risk and must be considered in post-intervention procedures.

Overall, this work demonstrates that the transition to electric mobility requires revisiting ventilation and suppression design philosophies in underground facilities. The findings emphasise that fire-safety engineering for BEVs cannot rely solely on traditional metrics developed for ICEVs, because the interplay among fire duration, ventilation intensity, and confined geometries creates behaviour that differs meaningfully from that of conventional vehicles. The study therefore contributes new data and modelling insight that support the refinement of design scenarios, risk assessments, and performance-based safety evaluations in modern parking infrastructures.

Author Contributions: Conceptualisation, D.P.; methodology, E.L. and D.P.; software, E.L.; validation, E.L.; formal analysis, D.P.; investigation, E.L. and D.P.; data curation, E.L.; writing—original draft preparation, E.L. and D.P. All authors have read and agreed to the published version of the manuscript.

Funding: This research received no external funding.

Data Availability Statement: The raw data supporting the conclusions of this article will be made available by the authors on request.

Conflicts of Interest: The authors declare no conflict of interest.

Abbreviations

ICEVs	Internal Combustion Engine Vehicles
EV	Electric Vehicle
MHEVs	Mild Hybrid EV
HEVs	Hybrid EV
PHEVs	Plug-in Hybrid EV
BEVs	Battery EV
LIB	Li-Ion Battery
BMS	Battery Management System
HRR	Heat Release Rate
FDS	Fire Dynamics Simulator
SMW	Smokeview
CFD	Computational Fluid Dynamics
HRRPUA	Heat Release Rate Per Unit Area

References

1. Guo, H.; Yang, Z.; Zhang, P.; Gao, Y.; Zhang, Y. Experimental Investigation on Fire Smoke Temperature under Forced Ventilation Conditions in a Bifurcated Tunnel with Fires Situated in a Branch Tunnel. *Fire* **2023**, *6*, 473. [CrossRef]
2. Sturm, P.; Fößleitner, P.; Fruhwirt, D.; Galler, R.; Wenighofer, R.; Heindl, S.F.; Krausbar, S.; Heger, O. Fire tests with lithium-ion battery electric vehicles in road tunnels. *Fire Saf. J.* **2022**, *134*, 103695. [CrossRef]
3. Lecocq, A.; Bertana, M.; Truchot, B.; Marlair, G. Comparison of the fire consequences of an electric vehicle and an internal combustion engine vehicle. In Proceedings of the 2. International Conference on Fires in Vehicles-FIVE 2012, Chicago, IL, USA, 27–28 September 2012; SP Technical Research Institute of Sweden: Boras, Sweden, 2012; pp. 183–194. [CrossRef]
4. Kang, S.; Kwon, M.; Choi, J.Y.; Choi, S. Full-scale fire testing of battery electric vehicles. *Appl. Energy* **2023**, *332*, 120497. [CrossRef]
5. Hodges, J.L.; Salvi, U.; Kapahi, A. Design fire scenarios for hazard assessment of modern battery electric and internal combustion engine passenger vehicles. *Fire Saf. J.* **2024**, *146*, 104145. [CrossRef]
6. Musso, L.; Donati, S.; Benelli, A.; Sobótka, M.; Bodak, B.; Pachnicz, M.; Fruhwirt, D.; Noone, P.; Knaup, L.; Zirker, C.; et al. Thermal runaway in lithium-ion batteries: Experimental insights from mechanical, thermal, and electrical stress tests. *Appl. Therm. Eng.* **2025**, *281*, 128661. [CrossRef]
7. Feng, X.; Ouyang, M.; Liu, X.; Lu, L.; Xia, Y.; He, X. Thermal runaway mechanism of lithium ion battery for electric vehicles: A review. *Energy Storage Mater.* **2018**, *10*, 246–267. [CrossRef]
8. Larsson, F.; Andersson, P.; Blomqvist, P.; Mellander, B.E. Toxic fluoride gas emissions from lithium-ion battery fires. *Sci. Rep.* **2017**, *7*, 10018. [CrossRef]
9. Sturk, D.; Rosell, L.; Blomqvist, P.; Tidblad, A.A. Analysis of Li-Ion Battery Gases Vented in an Inert Atmosphere Thermal Test Chamber. *Batteries* **2019**, *5*, 61. [CrossRef]
10. Yang, Y.; Wang, R.; Shen, Z.; Yu, Q.; Xiong, R.; Shen, W. Towards a safer lithium-ion batteries: A critical review on cause, characteristics, warning and disposal strategy for thermal runaway. *Adv. Appl. Energy* **2023**, *11*, 100146. [CrossRef]
11. Dessì, R.; Fruhwirt, D.; Papurello, D. A Study on Large Electric Vehicle Fires in a Tunnel: Use of a Fire Dynamics Simulator (FDS). *Processes* **2025**, *13*, 2435. [CrossRef]
12. Sun, P.; Bisschop, R.; Niu, H.; Huang, X. A Review of Battery Fires in Electric Vehicles. *Fire Technol.* **2020**, *56*, 1361–1410. [CrossRef]
13. Lee, S.; Choi, D.; Jeong, Y.; Moon, M.; Kwon, H.; Han, K.; Kim, H.; Im, H.; Park, Y.; Shin, D.; et al. Assessing fire dynamics and suppression techniques in electric vehicles at different states of charge: Implications for maritime safety. *Case Stud. Therm. Eng.* **2024**, *64*, 105474. [CrossRef]
14. Acar, O.; Honkavaara, E. A Review of Vehicles for Fire Suppression. *Preprints* **2024**. [CrossRef]
15. Considerations for ESS Fire Safety Consolidated Edison New York, NY. 2017. Available online: www.dnvgl.com (accessed on 10 December 2025).
16. Modern Vehicle Hazards in Parking Garages & Vehicle Carriers. Available online: https://www.nfpa.org/education-and-research/research/fire-protection-research-foundation/projects-and-reports/modern-vehicle-hazards-in-parking-garages-vehicle-carriers?utm_source=chatgpt.com (accessed on 10 December 2025).
17. Miechówka, B.; Węgrzyński, W. Systematic Literature Review on Passenger Car Fire Experiments for Car Park Safety Design. *Fire Technol.* **2025**, *61*, 2651–2688. [CrossRef]
18. Boehmer, H.; Klassen, M.; Olenick, S. Modern Vehicle Hazards in Parking Structures and Vehicle Carriers. 2020. Available online: www.nfpa.org/foundation (accessed on 10 December 2025).

19. Boehmer, H.R.; Klassen, M.S.; Olenick, S.M. Fire Hazard Analysis of Modern Vehicles in Parking Facilities. *Fire Technol.* **2021**, *57*, 2097–2127. [CrossRef]
20. Tohir, M.Z.M.; Spearpoint, M.; Fleischmann, C. Probabilistic design fires for passenger vehicle scenarios. *Fire Saf. J.* **2021**, *120*, 103039. [CrossRef]
21. Park, Y.; Ryu, J.; Ryou, H.S. Experimental Study on the Fire-Spreading Characteristics and Heat Release Rates of Burning Vehicles Using a Large-Scale Calorimeter. *Energies* **2019**, *12*, 1465. [CrossRef]
22. Li, D.; Zhu, G.; Zhu, H.; Yu, Z.; Gao, Y.; Jiang, X. Flame spread and smoke temperature of full-scale fire test of car fire. *Case Stud. Therm. Eng.* **2017**, *10*, 315–324. [CrossRef]
23. Lan, C.; Yingang, S.; Yuechen, C. Simulation of flames and smoke spreading in an underground garage under different ventilation conditions You may also like Design of Intelligent Garage Control System Based on Internet of Things. *J. Phys. Conf. Ser.* **2021**, *1736*, 012050. [CrossRef]
24. Brzezinska, D.; Bryant, P. Performance-Based Analysis in Evaluation of Safety in Car Parks under Electric Vehicle Fire Conditions. *Energies* **2022**, *15*, 649. [CrossRef]
25. Thermal Modeling of the Electric Vehicle Fire Hazard Effects on Parking Building on JSTOR. Available online: https://www.jstor.org/stable/27349122 (accessed on 13 November 2025).
26. Qiao, J.; Wang, Y.; Wang, H.; Li, X.; Wang, Y.; Wang, Y.; Zhang, H. Impact of ventilation strategies on the evolution of electric vehicle fire characteristics in ships. *Ocean. Eng.* **2025**, *317*, 120080. [CrossRef]
27. Stan, C.; Năstase, I.; Bode, F.; Calotă, R. Smoke and Hot Gas Removal in Underground Parking Through Computational Fluid Dynamics: A State of the Art and Future Challenges. *Fire* **2024**, *7*, 375. [CrossRef]
28. Meena, K.; Kumar, J.; Kumar, A.; Sharma, A.; Singh, D.K. *Study of Fire Dynamic Simulation of Electric Vehicle in Basement Parking*; National Fire Service College: Nagpur, India, 2025. [CrossRef]
29. Olenick, S.; Klassen, M.; Hussain, N. Classification of Modern Vehicle Hazards in Parking Structures & Systems-Ph II. 2024. Available online: www.nfpa.org/foundation (accessed on 10 December 2025).
30. Parking Garages and EVs. Available online: https://www.nfpa.org/news-blogs-and-articles/blogs/2024/07/12/parking-garages-and-evs?utm_source=chatgpt.com (accessed on 10 December 2025).
31. AMCRPS Underground Car Parks—Life Cycle Assessment | English Version | Enhanced Reader. Available online: https://projects.arcelormittal.com/media/4kspgix2/underground-car-parks-nl-part-2-lca-2021.pdf (accessed on 22 December 2025).
32. Thermal Properties Database of Building Materials and Technologies. Available online: https://www.researchgate.net/publication/357355874_Thermal_Properties_of_Building_Materials_-_Review_and_Database/citations (accessed on 22 December 2025).
33. Properties of Polymers | ScienceDirect. Available online: https://www.sciencedirect.com/book/monograph/9780080548197/properties-of-polymers (accessed on 11 December 2025).
34. E. M. Project Manager H Salley A Lindeman, "NUREG-2178, Vol.1, 'Refining And Characterizing Heat Release Rates From Electrical Enclosures During Fire (RACHELLE-FIRE), Volume 1: Peak Heat Release Rates and Effect of Obstructed Plume'". 2016. Available online: https://www.nrc.gov/docs/ML1611/ML16110A140.pdf (accessed on 22 December 2025).
35. Mishra, R.K.; Sharma, P.K.; Kumar, R. Experimental analysis of glass failure criteria under different thermal conditions. *Front. Therm. Eng.* **2024**, *4*, 1488206. [CrossRef]
36. E, J.; Xiao, H.; Tian, S.; Huang, Y. A comprehensive review on thermal runaway model of a lithium-ion battery: Mechanism, thermal, mechanical, propagation, gas venting and combustion. *Renew. Energy* **2024**, *229*, 120762. [CrossRef]

Disclaimer/Publisher's Note: The statements, opinions and data contained in all publications are solely those of the individual author(s) and contributor(s) and not of MDPI and/or the editor(s). MDPI and/or the editor(s) disclaim responsibility for any injury to people or property resulting from any ideas, methods, instructions or products referred to in the content.